

Structural and Spectroscopic Study of a Single Crystal of Lanthanum Aluminogallate, Doped with Neodymium

A. KAHN,* J. LECOMTE, J. THÉRY, AND D. VIVIEN

UA 302 CNRS, Chimie appliquée de l'état solide ENSCP,
11 rue Pierre et Marie Curie, 75321 Paris Cedex 05, France

Received February 29, 1988; in revised form April 25, 1988

The structure and optical properties of a neodymium activated lanthanum aluminogallate are described. This compound exhibits a promising laser behavior (5% Nd content, 1.059 and 1.08 μm fluorescence radiations, average lifetime of the Nd^{3+} ion excited state about 330 μs). The Czochralski grown single crystals have a hexagonal magnetoplumbite-like structure with space group $P6_3/mmc$, $Z = 2$, $a = 5.673(2)$ Å, $c = 22.32(1)$ Å and are shown to be nonstoichiometric (final R factor = 0.033, $R_w = 0.038$). The composition deduced from the structure refinement of the studied crystal is $\text{La}_{0.84}\text{Nd}_{0.04}\text{Mg}_{0.64}\text{Al}_{5.27}\text{Ga}_{6.13}\text{O}_{19}$. Aluminum and gallium are not randomly distributed on the available sites of the structure; Ga is rather found on tetrahedral or pseudo-tetrahedral sites, whereas Al is mainly sixfold coordinated. This has an effect on Nd^{3+} crystal field by increasing the L_n-L_n distances. The L_n deficiency (~ 0.9 instead of 1) is balanced by excess Al. L_n (La + Nd) is split on two sites with different local symmetry. This is suggested by X-ray structural investigation and confirmed by V-UV absorption and ESR spectroscopy, which reveal the occupation of both an axial 2d site (D_{3h} , about 80%) and a nonaxial satellite 6h position (C_{2v} , about 10%). This is consistent with previous results obtained for hexaaluminates and hexagallates. © 1988 Academic Press, Inc.

Introduction

Rare-earth hexaaluminates were first investigated for their luminescent properties by Philips Laboratories (1). Then our group succeeded in preparing single crystals of lanthanum hexaaluminate containing some neodymium (2) and was able to show the possible utilization of this material as an infrared high power laser (3). This compound, $\text{La}_{1-x}\text{Nd}_x\text{MgAl}_{11}\text{O}_{19}$, referred to as LNA, appears as a possible substitute for the YAG: Nd^{3+} , the most widely used solid-state laser, up to the present.

The structure of LNA is derived from that of magnetoplumbite $\text{PbFe}_{12}\text{O}_{19}$ (4) in which Al takes the place of Fe and a pair $\text{Pb}^{2+} + \text{Fe}^{3+}$ is replaced by $L_n^{3+} + \text{Mg}^{2+}$, to obtain the theoretical formula: $L_n\text{MgAl}_{11}\text{O}_{19}$.

In such a lattice, rare-earth ions are rather far from each other (distant from about 5.6 Å); this reduces the quenching effect of neighboring Nd atoms and allows a concentration in doping ions higher than in YAG (5 to 10% instead of 1%). Further reduction of the quenching effect could be achieved by lowering the crystal field at Nd^{3+} sites (5) through increasing the host lattice parameters. This can be obtained by

* To whom correspondence should be addressed.

substitution of gallium to aluminum in the lattice; unfortunately, lanthanum hexagallate cannot accept large amounts of Nd^{3+} (less than 20%). The mixed La, Nd hexagallate is a noncongruent melting compound, because Nd^{3+} is smaller than La^{3+} and the corresponding Nd hexagallate does not exist. Therefore the solution lies in a mixed aluminogallate compound where the presence of Al^{3+} allows the introduction of a convenient percentage of Nd^{3+} (6) to get interesting optical properties and successful crystal growth. The resulting phase is $\text{La}_{1-x}\text{Nd}_x\text{Mg}(\text{Al}_{1-y}\text{Ga}_y)_{11}\text{O}_{19}$, of which we were able to grow single crystals. One particular composition is described in this paper.

Two questions are to be solved, concerning this potential laser host material:

—First, what is the precise location of the optically active ion (Nd^{3+}), responsible of the laser effect.

—Second, is there a nonrandom distribution of gallium and aluminum on their available sites, which could explain the following observation made on powders: unit cell parameters do not vary continuously with the substitution of Ga^{3+} to Al^{3+} (7).

There are several limiting factors for X-ray structural study:

—The crystal growth of aluminogallates which provides crystals of rather poor quality, quality which decreases with increasing Ga amount. The crystal composition is not well established and is nonstoichiometric.

—The difficulty of identifying a very low Nd content (X-ray diffraction analysis cannot distinguish La from Nd).

—The presence of Mg^{2+} required to “stabilize” these compounds and to allow crystal growth (8); this ion cannot be distinguished from Al^{3+} , which has the same number of electrons.

In order to complete an X-ray investigation which provides an “average” structure, local information on Nd^{3+} was obtained from optical spectroscopy and ESR.

Experimental

Single crystals are grown by the Czochralski method, in an inert atmosphere (6). Owing to the noncongruency, the composition of the resulting crystals is not that of the starting mixture and is not quite homogeneous. The average composition corresponds to $y = 0.4$, referring to the upper formula (i.e., 60% Al and 40% Ga). Yet, electron probe microanalysis shows significant heterogeneities in the true composition of various crystalline domains, in the same bulk: the compound is clearly nonstoichiometric (vacancies in Ln, Mg, excess of Al, Ga, even the oxygen sublattice may have vacancies).

However, good crystalline platelets are available for X-ray and spectroscopic studies. Intensity measurements were collected from a single crystal on a Philips PW 1100 automatic diffractometer with $\text{MoK}\alpha$ radiation; all crystallographic data and procedures are given in Table I.

Owing to the crystal shape and to the presence of rather highly absorbing ions (La and Ga with $\lambda\text{MoK}\alpha = 0.7107$), absorption corrections were performed by the integration Gauss method, for all reflections with $F^2 > 3\sigma |F^2|$.

The refinement of the crystal structure was performed with a modified version of the O.R.F.L.S. least-squares program (9). The set of starting parameters consisted of atomic coordinates resulting from previous refinement of $\text{LaMgGa}_{11}\text{O}_{19}$ (10). This compound has a magnetoplumbite-like structure (space group $P6_3/mmc$), as shown in Fig. 1. The scattering factors for ionized atoms were taken from “International Tables for X-Ray Crystallography” (11). In-

TABLE I
CRYSTALLOGRAPHIC DATA AND PROCEDURE

Crystal symmetry	Hexagonal
Space group	$P6_3/mmc$; $Z = 2$
Unit cell	$a = b = 5.673(2) \text{ \AA}$, $c = 22.32(1) \text{ \AA}$ $V = 622.15 \text{ \AA}^3$
Density	$\rho_{\text{th}} = 5.2$
Absorption correction with	Gauss integration method
Linear absorption coefficient	$\mu = 149 \text{ cm}^{-1}$
Crystal size	$0.25 \times 0.26 \times 0.04 \text{ mm}$
Data collection	Phillips PW1100 four-circle diffractometer $\lambda\text{MoK}\alpha = 0.7107 \text{ \AA}$ Graphite monochromator $\theta/2\theta$ scan scanning speed: $0.02^\circ/\text{sec}$ $0 < h < 8, 0 < k < 8, 0 < l < 44$ $\sin \theta/\lambda_{\text{max}} = 0.99$ 3 standard reflections
Total of measured reflections	2250
No. of independent reflections	890; 580 with $F^2 > 3\sigma F^2 $
Diffusion factors	For fully ionized atoms From Cromer and Waber tables in (11)
R factor	0.033 with 577 reflections and 2 Ln positions
R_w	0.038 with unit weight in $R_w =$ $(\sum w(F_o - F_c)^2 / \sum w F_o ^2)^{1/2}$
Goodness of fit (S)	4.7
R factor	0.041 with 577 reflections and 1 Ln position ($R_w = 0.048$)
Residual electron density in the difference Fourier map is 1.7 e/\AA^3 with 2 Ln sites	

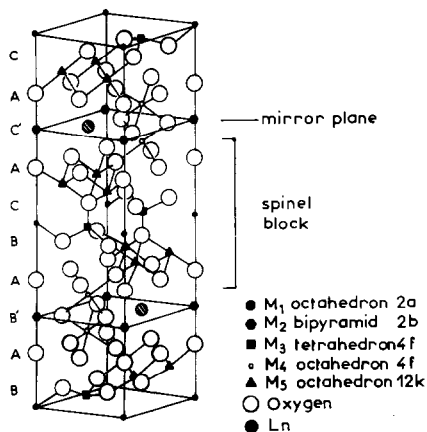


FIG. 1. Schematic view of the available sites for cations in the magnetoplumbite-like structure.

stead of Al^{3+} ($Z = 10$) or Ga^{3+} ($Z = 28$), an average atom M^{3+} was first introduced [$M = (\text{Mg} + 6 \text{Al} + 5 \text{Ga})/12$, $Z = 17.5$] in all available sites $M1$ to $M5$, which are given in Table II.

In the following, magnesium is assumed to behave as aluminum rather than gallium. This can be justified by noting the "inverse" structure of MgGa_2O_4 spinel, which corresponds to Mg mainly in octahedral sites and Ga in both octahedral and tetrahedral sites (12). One can then expect the same behavior of Mg in our compound.

Ln^{3+} was set on the theoretical 2d Wyck-off position, in the first refinement step.

TABLE II
STARTING VALUES FOR CATIONS PARAMETERS IN
P6₃/mmc Space Group

Site symmetry	Coord. number	<i>x</i>	<i>y</i> = 2 <i>x</i>	<i>z</i>	
<i>Ln</i>	2d	12	2/3	1/3	1/4
<i>M1</i>	2a	6	0	0	0
<i>M2</i>	2b	5	0	0	1/4
<i>M3</i>	4f	4	1/3	2/3	0.027
<i>M4</i>	4f	6	1/3	2/3	0.188
<i>M5</i>	12k	6	-0.168	-0.336	0.108

Refinement of the Structure

Taking into account the effect of thermal and occupancy factors on the values of calculated structure factors $F(hkl)$, we were able after a few steps of refinement to assign a more precise distribution of Al and Ga:

—*M2*, *M3*, and *M4* sites are filled by ions heavier in electrons than the average M^{3+} ion we introduced: it means that gallium is probably predominant on these sites.

—On *M1* site, a lighter electron density is found: Al is set on this position.

—The last *M5* position seems occupied by Al + Ga (see Table II).

At the same time, atomic coordinates were refined, together with further refinement of isotropic temperature factors. Lanthanum, set on a fixed position, exhibited a very high temperature factor, which had already been observed in compounds of the same family (8, 13). As the rare-earth has fixed coordinates, this strongly suggests that *Ln* is either shifted out of this 2d position and spread on a threefold 6h position, or is found on a second *Ln2* site. Therefore, both hypotheses were tested as refinement went on. The very strong correlation between coordinates, occupancy, and thermal factors for such sites did not allow a clear choice between these two possibilities at this stage.

Further refinement was performed with anisotropic thermal coefficients for “puzzling” atoms: *Ln1* and/or *Ln2* and *M2* in bipyramidal 2b site, all in the mirror planes of the structure.

For the *M2* fixed position (0, 0, 0.25), the *B* component along *z* is very large, this could account for a splitting into two equivalent 4e positions apart from the mirror plane, as already reported for similar compounds (8). This has been tested in the next refinement steps.

For *Ln1* and *Ln2* the thermal components in the mirror plane are also very large and probably cover the actual shift of the rare-earth ion out of its theoretical 2d position or the existence of a satellite site (6h), partly occupied. As we had reason to think that the *Ln* site(s) were not fully occupied, as previously mentioned in hexaaluminates (8), one more parameter was to be adjusted: occupancy factors for *Ln1* and *Ln2* positions. Then successive refinement steps always converged to nearly stable values of *Ln* total amount and *Ln1/Ln2* distribution on their respective sites, for the multisite description. The satellite site, however, has a weak occupancy and a very large anisotropic component in the mirror plane, and its existence is still questionable. For O₃ atom, lying in the same mirror planes as the rare-earth ions, a rather high thermal vibration was also detected.

Fourier and difference maps clearly show noticeable atomic shifts; with only one *Ln* introduced on a 6h site, residual electron density is detected on the theoretical *Ln1* site. With *Ln1* in 2d and *Ln2* in 6h positions, the final *R* value with 577 reflections is 0.033 ($R_w = 0.0038$), and the corresponding difference Fourier synthesis shows residual peaks and depressions not exceeding $1.7 \text{ e}\text{\AA}^{-3}$ (at $x = 0.625$, $y = 0.28$, $z = 0.25$).

The final set of atomic parameters is given in Table III, for the “multisite” description case (three very strong reflections at low Bragg angles were abandoned

TABLE III
FINAL SET OF ATOMIC PARAMETERS OF Nd: LANTHANUM ALUMINOGALLATE
($R = 0.033$ AND $R_w = 0.038$)

Type of atom	Wyckoff position	Coordination polyhedra	Coordinates			B thermal coefficient (isotropic equivalent)
			x	y	z	
$M1$ Al	2a	Octahedr.	0.	0.	0.	0.30(0)
$M2$ Ga	2b/4e	Tetrahydr. (ex bipy.)	0.	0.	0.241(0)	0.60(0)
$M3$ Ga	4f	Tetrahydr.	0.333	0.667	0.027(0)	0.35(0)
$M4$	4f	Octahedr.	0.333	0.667	0.188(0)	0.38(0)
0.6 Ga + 0.4 Al						
$M5$	12k	Octahedr.	-0.168(0)	-0.336	0.1085(0)	0.39(1)
0.4 Ga + 0.6 Al						
O1	4e		0.	0.	0.149(0)	0.26(4)
O2	4f		0.667	0.333	0.058(0)	0.27(4)
O4	12k		0.151(0)	0.302	0.053(1)	0.26(4)
O3	6h		0.183(0)	0.365	0.250	0.60(6)
O5	12k		0.506(0)	0.013	0.150(0)	0.27(4)
$Ln1$ (0.8)	2d		0.667	0.333	0.250	0.70(7)
$Ln2$ (0.1)	6h	($R = 0.033$)	0.723(2)	0.447	0.250	1.70(10)
or						
Ln (0.9)	6h	($R = 0.041$)	0.672(2)	0.344	0.250	1.10(7)

because of a strong extinction effect that could not be corrected). Values of U_{ij} mean square amplitude of vibrations are given in Table IV with the corresponding equivalent isotropic B factors. They clearly show that the satellite $Ln2$ site is not well defined, in spite of the better R factor corresponding to that description ($R = 0.041$ for one Ln site).

TABLE IV
MEAN SQUARE AMPLITUDE OF VIBRATIONS U_{ij}^a ($\times 10^{-5} \text{ \AA}^2$) FOR SOME PARTICULAR ATOMS AND EQUIVALENT ISOTROPIC THERMAL FACTORS FOR (A) ONE-SHIFTED Ln SITE ($R = 0.041$) or (B) TWO Ln SITES ($R = 0.033$)

Atomic site	U_{11}	U_{22}	U_{33}	U_{12}	U_{13}	U_{23}	B_{eq}
(A)							
$M2$ (4e)	709	709	1009	354	0	0	0.6
Ln (6h)	464	4114	757	2057	0	0	1.1
O3 (6h)	1550	244	252	122	0	0	0.7
(B)							
$M2$ (4e)	648	648	1009	324	0	0	0.6
$Ln1$ (2d)	1028	1028	757	514	0	0	0.7
$Ln2$ (6h)	733	8900	0	4450	0	0	1.7
O3 (6h)	1358	73	505	37	0	0	0.6

^a U_{ij} relevant relations are: $U_{11} = U_{22} = 2U_{12}$ for 2d, 2b/4h positions, $U_{22} = 2U_{12}$ for 6h positions in the general formula $T = \exp[-2\pi^2(U_{11}h^2a^{*2} + U_{22}k^2b^{*2} + U_{33}l^2c^{*2} + 2U_{12}hka^*b^* + 2U_{13} \dots)]$.

TABLE V
MAIN INTERATOMIC DISTANCES IN Nd-DOPED LANTHANUM ALUMINOGALLATE

Atomic site	Coordination number	<i>M</i> -O	Bond lengths (Å)	Predominant atom	Corresponding values in	
					La hexaaluminate Ref. (2)	La hexagallate Ref. (10)
<i>M1</i> (2a)	6	6 × O4	1.899(2)	Al	1.88	1.950
<i>M2</i> (2b) (4e)	4 + 1	3 × O3	1.806(4)	Ga	1.77	1.84
		O1	2.051(4)		1.99	2.08
		O1	2.458(7)		2.49	2.45
<i>M3</i> (4f)	4	3 × O4	1.881(3)	Ga	1.80	1.91
		O2	1.893(7)		1.81	1.92
<i>M4</i> (4f)	6	3 × O5	1.901(3)	0.6 Ga + 0.4 Al	1.86	1.93
		3 × O3	2.023(3)		1.97	2.07
<i>M5</i> (12k)	6	2 × O5	1.854(2)	0.4 Ga + 0.6 Al	1.84	1.90
		O1	1.879(3)		1.87	1.92
		O2	1.984(4)		1.95	2.03
		2 × O4	2.002(2)		1.97	2.05
<i>Ln</i> (2d)	12	6 × O5	2.729(3)			2.78
		6 × O3	2.841(2)			2.91
<i>Ln</i> (6h)	8 + 4	2 × O3	2.394(12)		2.30	
		4 × O5	2.623(5)		2.66	
		2 × O3	2.865(9)		2.71	
		2 × O5	3.085(10)		2.75	
		2 × O3	3.348(14)		2.89	

Description and Discussion of the Structure

From the final set of atomic coordinates, main interatomic distances and angles have been computed in order to describe the coordination polyhedra for the various cations. These values are reported in Table V.

The distribution of Al and Ga on the available sites is then confirmed, even if bond-length considerations are not highly reliable in such distorted polyhedra: *M*-O distances in *MO4* and *MO6* polyhedra, with *M* = Al, Mg, Ga, are found in the literature, for rather regular tetrahedra and octahedra. In our compound, only average *M*-O bond-lengths could be compared to the reference values. However, these main interatomic distances are compared to the

ones found in the corresponding hexaaluminate and hexagallate (2, 10, 14).

In this magnetoplumbite-like structure, it is revealed that gallium ions have a preferred location in the tetrahedral sites, whereas aluminum is found in octahedral environment. The shift of the *M2* atom out of its theoretical 2b position, brings along a distortion of the bipyramidal site (fivefold coordination) into a tetrahedron, more favorable to gallium. As gallium total occupancy is higher than the available tetrahedral positions, some extra gallium is also found in octahedra other than aluminum, particularly in the *M4* sites close to the mirror plane containing *Ln*³⁺ ions.

Rare-earth ions are probably shared between the theoretical twelve-coordinated site *Ln1* and a shifted *Ln2* site, with a lower coordination number (*n* = 8), not very well

TABLE VI
ACTUAL OCCUPANCY OF CATIONIC SITES

Site ^a	% Ga	% Al + Mg	% Ln
M1 2a	Oct.	12(2)	88
M2 2b	Tet.	91(3)	9
M3 4f	Tet.	78(3)	22
M4 4f	Oct.	63(3)	37
M5 12k	Oct.	38(4)	62
La1 2d			78(3)
La2 6h			10(1)
			$\Sigma = 88(4)$

^a *M* is an average ion: 6 Al + Mg + 5 Ga (*Z* = 17.5 electrons).

defined (Fig. 2). The total amount of Ln^{3+} is less than one per formula unit. Clearly, *Ln1* and *Ln2* sites cannot both be occupied in the same unit cell. This description accounts for some kind of static disorder (due to the crystal growth process?). Either *Ln1* or *Ln2* is occupied, and as *Ln2* is a threefold site, it is reasonable to think that one only of the three equivalent positions is occupied at once, in a unit-cell mirror.

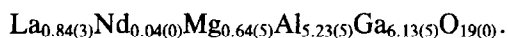
A check for local order between occupied and vacant sites for *Ln* atoms was performed by mean of X-ray diffuse scattering and gave a negative result, whereas such a local order exists in some of the corresponding hexaaluminates (8).

The final distribution of cations is given in Table VI and allows an estimation of the crystal composition:

$$\left. \begin{array}{l} \text{Al + Mg} \quad 5.87(5) \\ \text{Ga} \quad 6.13(5) \\ \text{La + Nd} \quad 0.88(3) \end{array} \right\} \begin{array}{l} \text{per} \\ \text{unit} \\ \text{formula} \end{array}$$

It is known from electron probe microanalysis of the crystal that Nd^{3+} represents 4.6% of total Ln^{3+} . We can then deduce the magnesium content to balance the formula, if we assume an oxygen lattice without vacancies (this could not be detected by refining occupancy factors of oxygen in such a disordered material). The approxi-

mate composition of the studied crystal is then about:



This crystallographic investigation of Nd-doped lanthanum aluminogallate has given an answer to some of the questions arising on this compound: Gallium and aluminum are not statistically distributed in the lattice, since gallium is rather found on the tetra- or pseudotetrahedral sites, whereas aluminum is found in sixfold coordinated positions. Some disorder remains in the location of these ions, as there are more gallium ions than available tetracoordinated sites. This is consistent with the expected behavior of these ions in the given magnetoplumbite-like structure.

Rare-earth ions are spread over two different sites, one with an axial symmetry on the theoretical 2d Wyckoff position, the other (6h) of lower symmetry with a lower occupancy factor. This result obtained on aluminogallates has already been mentioned for both *Ln* hexaaluminates (8) and hexagallates (10), but the respective occupancy of both sites varies according to the type of compound.

The question of whether La and Nd have a preferential location on these two sites cannot be answered by X-ray diffraction approach. Therefore, a spectroscopic study of Nd^{3+} was undertaken to get complementary information on the active ion location in the host lattice.

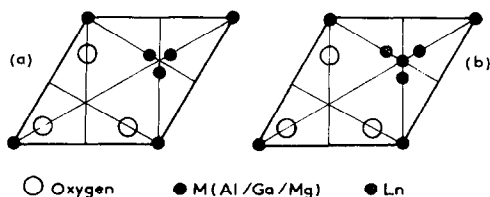


FIG. 2. Distribution of rare-earth ions in the mirror planes of a MP structure: (a) *Ln1* site; (b) *Ln1* + *Ln2* sites.

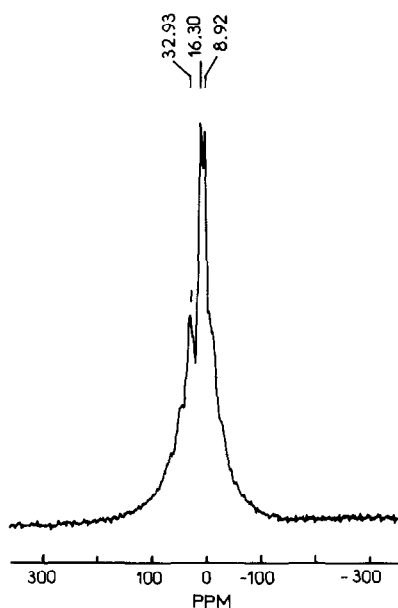


FIG. 3. MAS-NMR spectrum of ^{27}Al in Nd:lanthanum aluminogallate.

Spectroscopic Investigations

Optical absorption, fluorescence, and ESR for Nd^{3+} , on one hand, and MAS-NMR for ^{27}Al , on the other, provide useful details on the local environment of cations in this aluminogallate. These studies were performed on crystals of the same origin as the one studied by X-rays.

1. MAS-NMR Spectroscopy of ^{27}Al

Spectroscopic investigation was previously performed on polycrystalline samples of a series of La aluminogallates with variable Al/Ga ratios (14).

MAS-NMR of ^{27}Al in this family of compounds allows a clear detection of Al environment in the structure: the characteristic chemical shifts are well known for $[\text{AlO}_4]$ (55–80 ppm) and $[\text{AlO}_6]$ (0–20 ppm) polyhedra.

On crushed single crystals, MAS-NMR

spectra were obtained with a Bruker CXP-400 spectrometer (Fig. 3). A group of lines in the range 0–15 ppm is characteristic of Al in sixfold coordination, whereas no lines are detected in the region 60–80 ppm. It can then be deduced that, in the crystal lattice, tetrahedral sites are not occupied by Al (but by Ga and possibly some Mg, when there is a mixed occupancy, as in $M3$ site).

This qualitative test confirms the preference of Ga and Al for coordination 4 and 6, respectively, as it has already been shown in the X-ray structure determination. One can also note that there is no extra peak which could be assigned to Al in fivefold coordination.

2. ESR Study of Nd^{3+} Ion

The Nd^{3+} electronic configuration is $4f^3$; the ground state is $^4I_{9/2}$. Dilution of Nd (4.6%) prevents magnetic interaction between neighboring active ions which would broaden the ESR lines.

ESR spectra were recorded, at 20 K, on a Bruker ER220D X-band spectrometer equipped with an Oxford ESR9 cryostat. Cryogenic conditions were required since the spin lattice relaxation time for Nd^{3+} is very short at room temperature.

Angular dependence of the ESR spectra is obtained through rotating a crystal (size: $3 \times 2 \times 0.5$ mm) with respect to the static magnetic field B_0 . Two main directions give useful information on neodymium environment:

B_0 is \parallel to the c axis of the crystal (Fig. 4). A strong signal is detected. It corresponds to the position where the ESR line is the narrowest, with maximum intensity and minimum field position ($g = 3.894$). This clearly shows that the c direction is one of the axes of the g tensor for Nd^{3+} ion. At low temperature, only the lowest Kramers doublet of $^4I_{9/2}$ is populated and Nd^{3+} behaves as an $S = 1/2$ system.

Hyperfine lines are also seen on the spec-

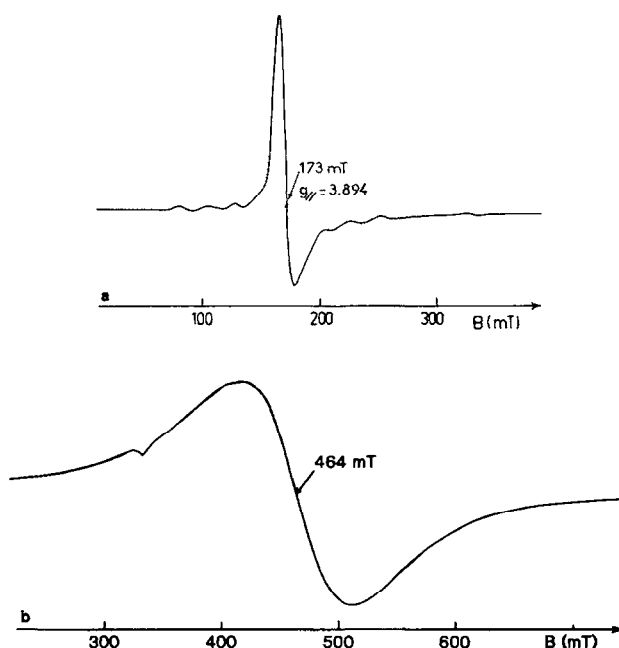


FIG. 4. ESR spectra of Nd^{3+} at low temperature: (a) magnetic field $B_0 \parallel$ to c axis; (b) magnetic field perpendicular to c axis angular, rotation in the (a,b) plane.

tra, apart from the central line: they arise from interactions with ^{143}Nd and ^{145}Nd isotopes (natural abundance 12 and 8%, respectively) both with $I = 7/2$. One hyperfine constant (A^{143}) is determined as $A_{\parallel} = 24.6$ mT. The other can be calculated, the two hyperfine constants being in the ratio of the nuclear g factors of the two corresponding Nd isotopes: $g_{143}/g_{145} = 1.63$.

When B_0 rotates from the c direction to that of (a,b) plane, the line moves toward higher fields and becomes broader. For $B_0 \perp c$, $g_{\perp} = 1.5$.

For $B_0 \perp c$, a rotation is performed in the (a,b) plane. With a true axial site (Nd^{3+} in 2d theoretical position), the corresponding ESR spectra would be a single line, for which the position should be independent of the rotation angle. Here, a broad asymmetric line only is observed, varying in position, height, and width through the rotation. The g factor ranges from 1.504 to 1.444, with a 60° angular periodicity. There

is no clear evidence of several lines but the asymmetry suggests that this line could have several components (Fig. 4).

We may then assume that Nd is in a 6h, nonaxial site, but very close to the axial position. This situation would result in three ESR lines arising from the three equivalent 6h sites in a mirror plane, for which the in-plane g tensor axes are rotated by 120° with respect to each other. However, owing to the broadening of each individual line, only the envelope is observed. Computer simulation of such ESR spectra shows that the center of the resulting line does present a 60° periodicity.

Owing to the linewidth (70 to 100 mT) of the "perpendicular" spectrum, hyperfine satellites are not resolved. Therefore A_{\perp} is computed from the spectrum recorded at an angle of $\theta = 20^\circ$ from c , using the classical formula:

$$(g^2 A^2)_{\theta} = (g^2 A^2)_{\parallel} \cos^2 \theta + (g^2 A^2)_{\perp} \sin^2 \theta.$$

TABLE VII
SPIN HAMILTONIAN PARAMETERS OF Nd³⁺
IN Ln ALUMINOGALLATE

	$B_{\parallel} (\theta = 0^\circ)$	$B_{\perp} (\theta = 90^\circ)$
g	3.89	1.504–1.444
ΔB line width	12 mT	70–100 mT
A143 hyperfine constant	24.6	58 mT
A145	15.4	

$A_{20^\circ} = 26$ mT; hence $A_{\perp} = 58$ mT, a roughly approximated value.

The resulting spin Hamiltonian parameters are given in Table VII. From these results no evidence is given of a second site for neodymium. An explanation is that there is only 4% Nd on the rare-earth sites, and if the second site is weakly occupied it corresponds to a nondetectable amount of neodymium.

3. Visible–UV Absorption Spectroscopy

Optical absorption of a single crystal (size: $4 \times 4 \times 1$ mm) was recorded down to 6 K on a Beckman UV 5270 spectrometer fitted with a helium flow cryostat, in the wavelength range 200–1200 nm. The light beam was along the c crystal axis.

Among the 41 degenerate states of the Nd³⁺ configuration, the $^2P_{1/2}$ level is of special interest. The transition from the $^4I_{9/2}$ ground level to $^2P_{1/2}$ occurs in an easily observed spectral range (430 nm). This level is not split by the crystal field, since $J + 1/2 = 1$. Therefore five lines are expected for one given Nd site, corresponding to the possible transitions from the five Stark levels of $^4I_{9/2}$ to $^2P_{1/2}$.

Decreasing temperature keeps the electron population to the lowest Kramers doublet of the $^4I_{9/2}$ ground state, and reduces the number of lines to one per site.

For our crystal, at liquid helium temperature, two lines are present, at 427 and 430 nm (Fig. 5). This is attributed to a distribution of Nd on two different sites at least,

one being significantly more populated (430 nm). Assuming that the separation between the peaks is related to the nephelauxetic effect (15), the peak at higher wavelength should correspond to a higher coordination number (probably 12) and large Nd–oxygen distances. Therefore, the 430-nm line is assigned to the 2d lanthanide site; instead of 12 oxygen nearest neighbors for Nd in the axial site, Nd in the 6h site has eight close and four further neighbors; the actual coordination is lowered and the corresponding line appears at a lower wavelength (427 nm).

This is clear evidence of the multisite character of the neodymium ion, even if intensities cannot be connected to the real occupancy of both sites, contrary to ESR spectra, where line intensities are roughly proportional to the amount of Nd in the corresponding sites.

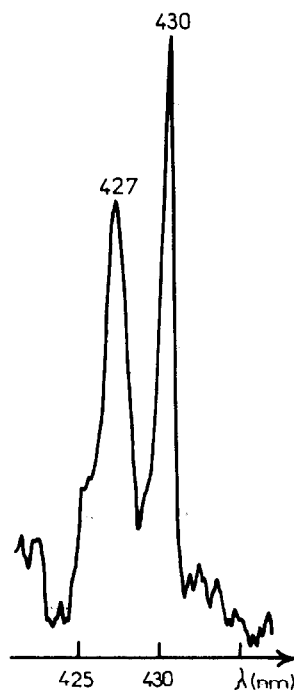


FIG. 5. $^2P_{1/2}$ transition in V–UV absorption spectra of Nd³⁺ at low temperature.

4. Fluorescence Spectrum and Lifetime

The fluorescence spectrum of the crystal ${}^4F_{3/2} \rightarrow {}^4I_{11/2}$ transition have been recorded under excitation with the 577-nm line of a mercury lamp. It shows two broad bands peaking at 1.059 and 1.08 μm . Further details relevant to that spectrum are given elsewhere (6).

Nd fluorescence lifetime measurements have been performed under 590 nm excitation with a dye laser pumped by a nitrogen laser. The room-temperature fluorescence decay is exponential and the average lifetime obtained on three different samples of the crystal is about 330 μsec . Knowing that the fluorescence lifetime decreases with increasing neodymium content, this parameter in aluminogallates shows that these compounds deserve further investigation. In the considered compound, a point of interest is the neodymium lifetime that does not vary with temperature between 294 and 616 K. Similar behavior is observed (16) for the laser material YAG: Nd³⁺. This means that the nonradiative desexcitation of the ${}^4F_{3/2}$ level is negligible compared to the radiative one, and also that energy migration and quenching of Nd³⁺ excitation at killer centers do not occur in that temperature range.

Conclusion

As a conclusion of this structural and spectroscopic investigation of Nd-doped lanthanum aluminogallate, two particular points of interest have been clarified, in the purpose of possible laser application of this new material:

Aluminum and gallium have specific positions in the lattice: all tetrahedral or pseudo-tetrahedral sites are mainly occupied by Ga³⁺ whereas Al³⁺ is essentially found in octahedral sites. Of course total order is not established, and depends on the actual Al/Ga ratio and on the crystal perfection. However, this distribution of ions,

with Ga close to the mirror planes of the structure, seems favorable to modify the crystal field around the rare-earth located in these planes, by increasing the Nd-Nd distance in the host lattice. The resulting composition deduced from the structure refinement of the studied crystal is La_{0.84}Nd_{0.04}Mg_{0.64}Al_{5.27}Ga_{6.13}O₁₉.

The Nd³⁺ ion, optically active in the laser emission, is found on two sites at least, one very close to the axial 2d Wyckoff position (D_{3h}), the other on a satellite 6h position (C_{2v}), with much lower occupancy (this site is not observed by ESR because of this weak occupancy). There is no apparent segregation between Nd and La on the two available sites.

The optical behavior of this rare-earth aluminogallate shows radiative transitions with $\lambda = 1.059$ and 1.080 μm , lifetime of the excited state equals 330 μsec , and justifies the tests on laser properties now in progress in our laboratory.

Acknowledgments

Acknowledgments are due to Dr. B. Ferrand (CENG-LETI, Grenoble) for growing the single crystals, Dr. F. Taulelle (CNRS, Paris) for MAS-NMR investigation and Dr. J. Barrie (UCLA, Los Angeles) for lifetime measurements.

References

1. J. P. M. J. VERSTEGEN, *J. Solid State Chem.* **7**, 468 (1973).
2. A. KAHN, A. M. LEJUS, M. MADSAK, J. THÉRY, D. VIVIEN, AND J. C. BERNIER, *J. Appl. Phys.* **52**, 6864 (1981).
3. L. D. SCHEARER, M. LEDUC, D. VIVIEN, A. M. LEJUS, AND J. THÉRY, *IEEE J. Quantum Electr.* **22**, 713 (1986).
4. V. ADELKOLD, *Arkiv Kemi. Mineral. Geol. A* **12**, 1 (1938).
5. F. AUZEL, *Mater. Res. Bull.* **14**, 223 (1979).
6. D. LEFÈVRE, J. THÉRY, D. VIVIEN, B. FERRAND, Y. GRANGE, AND F. AUZEL, *J. Phys.* **48**, C7 467 (1987).
7. D. LEFÈVRE, J. THÉRY, AND D. VIVIEN, *J. Amer. Ceram. Soc.* **69**, C289 (1986).

8. M. GASPERIN, M. C. SAINÉ, A. KAHN, F. LAVILLE, AND A. M. LEJUS, *J. Solid State Chem.* **54**, 61 (1984).
9. W. R. BUSING, K. O. MARTIN, AND H. A. LEVY, "O.R.F.L.S. Least Squares Program," Oak Ridge, 1972. [French adaptation]
10. D. LEFÈVRE, A. KAHN, AND J. THÉRY, *C.R. Acad. Sci. Paris, Ser. III* **300**, 263 (1985).
11. "International Tables for X-Ray Crystallography" (J. A. Ibers and W. C. Hamilton, Ed.), Vol. 4, Kynoch Press, Birmingham (1973).
12. M. HUBER, *J. Chim. Phys.* **57**, 202 (1960).
13. S. C. ABRAHAMS, P. MARSH, AND C. D. BRANDLE, *J. Chem. Phys.* **86**, 4224 (1987).
14. D. LEFÈVRE, Thèse de doctorat, Université Paris VI (1986).
15. P. CARO AND J. DEROUET, *Bull. Soc. Chim.* **1**, 46 (1972).
16. A. A. KAMINSKII, "Laser Compounds" (English translation), Springer-Verlag, Berlin/Heidelberg/New York (1981).